

# The strong $\Lambda_b NB$ and $\Lambda_c ND$ vertices

K. Azizi<sup>a \*</sup>, Y. Sarac<sup>b †</sup>, H. Sundu<sup>c ‡</sup>

<sup>a</sup> Department of Physics, Doğuş University, Acıbadem-Kadıköy, 34722 Istanbul, Turkey

<sup>b</sup> Electrical and Electronics Engineering Department, Atilim University, 06836 Ankara, Turkey

<sup>c</sup> Department of Physics, Kocaeli University, 41380 Izmit, Turkey

## Abstract

We investigate the strong vertices among  $\Lambda_b$ , nucleon and  $B$  meson as well as  $\Lambda_c$ , nucleon and  $D$  meson in QCD. In particular, we calculate the strong coupling constants  $g_{\Lambda_b NB}$  and  $g_{\Lambda_c ND}$  for different Dirac structures entered the calculations. In the case of  $\Lambda_c ND$  vertex, the result is compared with the only existing prediction obtained at  $Q^2 = 0$ .

PACS number(s): 13.30.-a, 13.30.Eg, 11.55.Hx

---

\*e-mail: kazizi@dogus.edu.tr

†e-mail: ysoymak@atilim.edu.tr

‡e-mail: hayriye.sundu@kocaeli.edu.tr

# 1 Introduction

The last decade has witnessed to significant experimental progresses on the spectrum and decay products of the hadrons containing heavy quarks. These progresses have been stimulated the theoretical interests on the spectroscopy of these baryons via various methods (for some of them see [1–11] and references therein). For a better understanding of the heavy flavor physics, it is also necessary to gain deeper insight into the radiative, strong and weak decays of the baryons containing a heavy quark. For some of the related studies, see [12–28] and references therein.

The strong coupling constants are the main ingredients of the strong interactions of the heavy baryons. To improve our understanding on the strong interactions among the heavy baryons and other hadrons and gain knowledge about the nature and structure of the participated particles, one needs the accurate determinations of these coupling constants. In the present study, we calculate the strong coupling constants  $g_{\Lambda_b NB}$  and  $g_{\Lambda_c ND}$  within the framework of the QCD sum rule [29] as one of the most powerful and applicable tools to hadron physics. These coupling constants are relevant in the bottom and charmed mesons clouds description of the nucleon which may be used to explain exotic events observed by different Collaborations. Besides, in order to exactly determine the modifications in the masses, decay constants and other parameters of the  $B$  and  $D$  mesons in nuclear medium we should immediately consider the contributions of the baryons  $\Lambda_{b[c]}$  and  $\Sigma_{b[c]}$  in the medium produced by the interactions of  $B$  and  $D$  mesons with the nucleon, viz.

$$\begin{aligned} B^-(b\bar{u}) + p( uud) \text{ or } n( udd) &\rightarrow \Lambda_b^0( udb) \text{ or } \Sigma_b^-( ddb), \\ D^0(c\bar{u}) + p( uud) \text{ or } n( udd) &\rightarrow \Lambda_c^+, \Sigma_c^+( udc) \text{ or } \Sigma_c^0( ddc). \end{aligned} \quad (1)$$

Hence, we need to know the exact values of the strong coupling constants  $g_{\Lambda_b NB}$ ,  $g_{\Lambda_c ND}$ ,  $g_{\Sigma_b NB}$  and  $g_{\Sigma_c ND}$  entering the Born term in the calculations [30–34]. Note that, among these couplings, we have only one approximate prediction for the strong coupling  $g_{\Lambda_c ND}$  in the literature calculated at zero transferred momentum square taking the Borel masses in the initial and final channels as the same [19]. We shall also refer to a pioneering work [35], which estimates the strong coupling constant  $g_{NKA}$ . Here we should also stress that our work on the calculation of the strong coupling constants  $g_{\Sigma_b NB}$  and  $g_{\Sigma_c ND}$  is in progress.

The layout of this article is as follows. The next section presents the details of the calculations of the strong coupling constants under consideration. In section 3, we numerically analyze the sum rules obtained and discuss the results.

## 2 The strong coupling form factors

The purpose of the present section is to give the details of the calculations of the coupling form factors  $g_{\Lambda_b NB}(q^2)$  and  $g_{\Lambda_c ND}(q^2)$ . The values of these form factors at  $Q^2 = -q^2 = -m_{B[D]}^2$  give the strong coupling constants among the participating particles. To fulfill this aim, the starting point is the usage of the following three-point correlation function:

$$\Pi(p, p', q) = i^2 \int d^4x \int d^4y e^{-ip \cdot x} e^{ip' \cdot y} \langle 0 | \mathcal{T} (J_N(y) J_{B[D]}(0) \bar{J}_{\Lambda_{b[c]}}(x)) | 0 \rangle, \quad (2)$$

where  $\mathcal{T}$  denotes the time ordering operator and  $q = p - p'$  is transferred momentum. The three-point correlation function contains interpolating currents that can be written in terms of the quark field operators as:

$$\begin{aligned} J_{\Lambda_b[\Lambda_c]}(x) &= \varepsilon_{abc} u^{aT}(x) C \gamma_5 d^b(x) b[c]^c(x), \\ J_N(y) &= \varepsilon_{ijk} \left( u^{iT}(y) C \gamma_\mu u^j(y) \right) \gamma_5 \gamma_\mu d^k(y), \\ J_{B[D]}(0) &= \bar{u}(0) \gamma_5 b[c](0), \end{aligned} \quad (3)$$

where  $C$  is the charge conjugation operator.

The calculation of the three-point correlation function is made via following two different ways. In the first way, which is called as hadronic side, one calculates it in terms of the hadronic degrees of freedom. In the second way, which is called as OPE side, it is calculated in terms of quark and gluon degrees of freedom using the operator product expansion in deep Euclidean region. These two sides are then matched to obtain the QCD sum rules for the coupling form factors. We apply a double Borel transformation with respect to the variables  $p^2$  and  $p'^2$  to both sides to suppress the contributions of the higher states and continuum.

The calculation of the hadronic side of the correlation function requires its saturation with complete sets of appropriate  $\Lambda_b[\Lambda_c]$ ,  $B[D]$  and  $N$  hadronic states having the same quantum numbers as their interpolating currents. This step is followed by performing the four-integrals over  $x$  and  $y$ , which leads to

$$\begin{aligned} \Pi(p, p', q) &= \frac{\langle 0 | J_N | N(p') \rangle \langle 0 | J_{B[D]} | B[D](q) \rangle \langle \Lambda_b[\Lambda_c](p) | \bar{J}_{\Lambda_b[\Lambda_c]} | 0 \rangle}{(p^2 - m_{\Lambda_b[\Lambda_c]}^2)(p'^2 - m_N^2)(q^2 - m_{B[D]}^2)} \\ &\times \langle N(p') B[D](q) | \Lambda_b[\Lambda_c](p) \rangle + \dots, \end{aligned} \quad (4)$$

where  $\dots$  represents the contributions coming from the higher states and continuum. The matrix elements in this equation are parameterized as

$$\begin{aligned} \langle 0 | J_N | N(p') \rangle &= \lambda_N u_N(p', s'), \\ \langle \Lambda_b(p) | \bar{J}_{\Lambda_b[\Lambda_c]} | 0 \rangle &= \lambda_{\Lambda_b[\Lambda_c]} \bar{u}_{\Lambda_b[\Lambda_c]}(p, s), \\ \langle 0 | J_{B[D]} | B[D](q) \rangle &= i \frac{m_{B[D]}^2 f_{B[D]}}{m_u + m_{b[c]}}, \\ \langle N(p') B[D](q) | \Lambda_b[\Lambda_c](p) \rangle &= g_{\Lambda_b N B[\Lambda_c N D]} \bar{u}_N(p', s') i \gamma_5 u_{\Lambda_b[\Lambda_c]}(p, s), \end{aligned} \quad (5)$$

where  $\lambda_N$  and  $\lambda_{\Lambda_b[\Lambda_c]}$  are the residues; and  $u_N$  and  $u_{\Lambda_b[\Lambda_c]}$  are the spinors for the nucleon and  $\Lambda_b[\Lambda_c]$  baryon, respectively. In the above equations,  $f_{B[D]}$  is the leptonic decay constant of  $B[D]$  meson and  $g_{\Lambda_b N B[\Lambda_c N D]}$  is the strong coupling form factor among  $\Lambda_b[\Lambda_c]$ ,  $N$  and  $B[D]$  particles. The use of Eqs. (5) in Eq. (4) is followed by summing over the spins of the  $N$  and  $\Lambda_b[\Lambda_c]$  baryons, i.e.

$$\begin{aligned} \sum_{s'} u_N(p', s') \bar{u}_N(p', s') &= \not{p}' + m_N, \\ \sum_s u_{\Lambda_b[\Lambda_c]}(p, s) \bar{u}_{\Lambda_b[\Lambda_c]}(p, s) &= \not{p} + m_{\Lambda_b[\Lambda_c]}. \end{aligned} \quad (6)$$

As a result, we have

$$\begin{aligned}
\Pi(p, p', q) &= i^2 \frac{m_{B[D]}^2 f_{B[D]}}{m_{b[c]} + m_u} \frac{\lambda_N \lambda_{\Lambda_b[\Lambda_c]} g_{\Lambda_b N B[\Lambda_c N D]}}{(p^2 - m_{\Lambda_b[\Lambda_c]}^2)(p'^2 - m_N^2)(q^2 - m_{B[D]}^2)} \\
&\times \left\{ (m_N m_{\Lambda_b[\Lambda_c]} - m_{\Lambda_b[\Lambda_c]}^2) \gamma_5 + (m_{\Lambda_b[\Lambda_c]} - m_N) \not{p} \gamma_5 + \not{q} \not{p} \gamma_5 - m_{\Lambda_b[\Lambda_c]} \not{q} \gamma_5 \right\} \\
&+ \dots
\end{aligned} \tag{7}$$

The final form of the hadronic side of the correlation function is obtained after the application of the double Borel transformation with respect to the initial and final momenta squared, viz.

$$\begin{aligned}
\widehat{\Pi}(q) &= i^2 \frac{m_{B[D]}^2 f_{B[D]}}{m_{b[c]} + m_u} \frac{\lambda_N \lambda_{\Lambda_b[\Lambda_c]} g_{\Lambda_b N B[\Lambda_c N D]}}{(q^2 - m_{B[D]}^2)} e^{-\frac{m_{\Lambda_b[\Lambda_c]}^2}{M^2}} e^{-\frac{m_N^2}{M'^2}} \\
&\times \left\{ (m_N m_{\Lambda_b[\Lambda_c]} - m_{\Lambda_b[\Lambda_c]}^2) \gamma_5 + (m_{\Lambda_b[\Lambda_c]} - m_N) \not{p} \gamma_5 + \not{q} \not{p} \gamma_5 - m_{\Lambda_b[\Lambda_c]} \not{q} \gamma_5 \right\} \\
&+ \dots,
\end{aligned} \tag{8}$$

where  $M^2$  and  $M'^2$  are Borel mass parameters.

The OPE side of the correlation function is calculated in deep Euclidean region, where  $p^2 \rightarrow -\infty$  and  $p'^2 \rightarrow -\infty$ . To proceed, the explicit expressions of the interpolating currents are inserted into the correlation function in Eq. (2). After contracting out all quark pairs via Wick's theorem we get

$$\begin{aligned}
\Pi(p, p', q) &= i^2 \int d^4 x \int d^4 y e^{-ip \cdot x} e^{ip' \cdot y} \varepsilon_{abc} \varepsilon_{ij\ell} \\
&\times \left\{ \gamma_5 \gamma_\mu S_d^{cj}(y-x) \gamma_5 C S_u^{biT}(y-x) C \gamma_\mu S_u^{ah}(y) \gamma_5 S_{b[c]}^{h\ell}(-x) \right. \\
&\quad \left. - \gamma_5 \gamma_\mu S_d^{cj}(y-x) \gamma_5 C S_u^{aiT}(y-x) C \gamma_\mu S_u^{bh}(y) \gamma_5 S_{b[c]}^{h\ell}(-x) \right\},
\end{aligned} \tag{9}$$

where  $S_{b[c]}^{i\ell}(x)$  represents the heavy quark propagator which is given by [36]

$$\begin{aligned}
S_{b[c]}^{i\ell}(x) &= \frac{i}{(2\pi)^4} \int d^4 k e^{-ik \cdot x} \left\{ \frac{\delta_{i\ell}}{\not{k} - m_{b[c]}} - \frac{g_s G_{i\ell}^{\alpha\beta}}{4} \frac{\sigma_{\alpha\beta}(\not{k} + m_{b[c]}) + (\not{k} + m_{b[c]}) \sigma_{\alpha\beta}}{(k^2 - m_{b[c]}^2)^2} \right. \\
&\quad \left. + \frac{\pi^2}{3} \langle \frac{\alpha_s G G}{\pi} \rangle \delta_{i\ell} m_{b[c]} \frac{k^2 + m_{b[c]} \not{k}}{(k^2 - m_{b[c]}^2)^4} + \dots \right\},
\end{aligned} \tag{10}$$

and  $S_u(x)$  and  $S_d(x)$  are the light quark propagators and are given by

$$\begin{aligned}
S_q^{ij}(x) &= i \frac{\not{x}}{2\pi^2 x^4} \delta_{ij} - \frac{m_q}{4\pi^2 x^2} \delta_{ij} - \frac{\langle \bar{q} q \rangle}{12} \left( 1 - i \frac{m_q}{4} \not{x} \right) \delta_{ij} - \frac{x^2}{192} m_0^2 \langle \bar{q} q \rangle \left( 1 - i \frac{m_q}{6} \not{x} \right) \delta_{ij} \\
&- \frac{i g_s G_{\theta\eta}^{ij}}{32\pi^2 x^2} [\not{x} \sigma^{\theta\eta} + \sigma^{\theta\eta} \not{x}] + \dots
\end{aligned} \tag{11}$$

The substitution of these explicit forms of the heavy and light quark propagators into Eq. (9) is followed by the usage of the following Fourier transformations in  $D = 4$  dimensions:

$$\begin{aligned}\frac{1}{[(y-x)^2]^n} &= \int \frac{d^D t}{(2\pi)^D} e^{-it \cdot (y-x)} i (-1)^{n+1} 2^{D-2n} \pi^{D/2} \frac{\Gamma(D/2-n)}{\Gamma(n)} \left(-\frac{1}{t^2}\right)^{D/2-n}, \\ \frac{1}{[y^2]^n} &= \int \frac{d^D t'}{(2\pi)^D} e^{-it' \cdot y} i (-1)^{n+1} 2^{D-2n} \pi^{D/2} \frac{\Gamma(D/2-n)}{\Gamma(n)} \left(-\frac{1}{t'^2}\right)^{D/2-n}.\end{aligned}\quad (12)$$

Then, the four- $x$  and four- $y$  integrals are performed in the sequel of the replacements  $x_\mu \rightarrow i \frac{\partial}{\partial p_\mu}$  and  $y_\mu \rightarrow -i \frac{\partial}{\partial p'_\mu}$ . As a result, these integrals turn into Dirac delta functions which are used to take the four-integrals over  $k$  and  $t'$ . Finally the Feynman parametrization and

$$\int d^4 t \frac{(t^2)^\beta}{(t^2 + L)^\alpha} = \frac{i\pi^2 (-1)^{\beta-\alpha} \Gamma(\beta+2) \Gamma(\alpha-\beta-2)}{\Gamma(2) \Gamma(\alpha) [-L]^{\alpha-\beta-2}}, \quad (13)$$

are used to perform the remaining four-integral over  $t$ .

The correlation function in OPE side is obtained in terms of different structures as

$$\Pi(p, p', q) = \Pi_1(q^2) \gamma_5 + \Pi_2(q^2) \not{p} \gamma_5 + \Pi_3(q^2) \not{q} \not{p} \gamma_5 + \Pi_4(q^2) \not{q} \gamma_5, \quad (14)$$

where each  $\Pi_i(q^2)$  function includes the contributions coming from both the perturbative and non-perturbative parts and can be written as

$$\Pi_i(q^2) = \int ds \int ds' \frac{\rho_i^{pert}(s, s', q^2) + \rho_i^{non-pert}(s, s', q^2)}{(s-p^2)(s'-p'^2)}. \quad (15)$$

The imaginary parts of the  $\Pi_i$  functions give the spectral densities  $\rho_i(s, s', q^2)$  appearing in the last equation, viz.  $\rho_i(s, s', q^2) = \frac{1}{\pi} \text{Im}[\Pi_i]$ . As examples, we present only the explicit forms of the spectral functions  $\rho_1^{pert}(s, s', q^2)$  and  $\rho_1^{non-pert}(s, s', q^2)$  corresponding to the Dirac structure  $\gamma_5$ , which are obtained as

$$\begin{aligned}\rho_1^{pert}(s, s', q^2) &= \left\{ -\frac{m_{b[c]} m_u s'^2}{64\pi^4 (q^2 - m_{b[c]}^2)} \Theta[L_1(s, s', q^2)] + \int_0^1 dx \int_0^{1-x} dy \frac{1}{64\pi^4 u^3} \right. \\ &\times \left[ 2m_{b[c]}^4 x^2 (1 + 3x^2 - y + 6xy - 4x) + m_{b[c]}^3 x (3m_d u (2x - 1) + m_u (3 + 2x^2 \right. \\ &- 3y - 5x - 2xy)) + 2m_{b[c]}^2 x (s(12x^4 + y^2 - y - 30x^3 + 36x^3 y - 6x + 20xy \\ &- 13xy^2 + 24x^2 - 55x^2 y + 24x^2 y^2) + q^2 xy (18x - 24xy + 7y - 12x^2 - 6) \\ &+ s' y (12x^3 + 7y - 4y^2 - 27x^2 + 36x^2 y + 18x - 43xy + 24xy^2 - 3)) \\ &+ 2s^2 u^2 x (10x^3 + 6x - 15xy + 2y - 16x^2 + 20x^2 y) + 2q^4 x^2 y^2 (10x^2 - 7y \\ &- 16x + 20xy + 6) + 2s'^2 y^2 u^2 (10x^2 - 3y - 12x + 20xy) - 4q^2 s' xy^2 (10x^3 \\ &+ 9y - 5y^2 - 24x^2 + 30x^2 y + 18x - 39xy + 20xy^2 - 4) + 2suy (q^2 x (32x^2 \end{aligned}$$

$$\begin{aligned}
& - 40x^2y - 20x^3 - 2y - 13x + 22xy + 1) + s'(20x^4 - 48x^3 + 60x^3y - y + y^2 \\
& - 8x + 27xy - 18xy^2 + 36x^2 - 86x^2y + 40x^2y^2)) + 3m_{b[c]}m_uu\left(q^2x(x+2y\right. \\
& - 3xy - 1) + sux(3x - 1) + s'u(3xy - x - y)) - m_{b[c]}m_u\left(q^2x(3x^2y - 3x^2\right. \\
& + 7y - 4y^2 + 6x - 10xy - 3xy^2 - 3) - sux(3x^2 - y - 6x - 6xy + 3) \\
& \left. - 3s'u(x^2y - x^2 + y - y + x - 3xy - xy^2))\right]\Theta[L_2(s, s', q^2)]\Big\}, \tag{16}
\end{aligned}$$

and

$$\begin{aligned}
\rho_1^{non-pert}(s, s', q^2) &= \left\{ \frac{1}{16\pi^2(m_{b[c]}^2 - q^2)} \left[ 2m_{b[c]}m_dm_u\langle\bar{d}d\rangle + \left( m_{b[c]}(3m_u^2 - 3m_dm_u - 2s') \right. \right. \right. \\
&+ m_d(4m_u^2 + s - s') + 2m_us')\langle\bar{u}u\rangle \Big] - \langle\alpha_s\frac{G^2}{\pi}\rangle \left[ \frac{m_{b[c]}m_uq^2s'^2}{192\pi^2(q^2 - m_{b[c]}^2)^4} \right. \\
&- \frac{9m_{b[c]}s'(m_d + m_u) + 2s'(q^2 - 2s + 5s')}{1152\pi^2(q^2 - m_{b[c]}^2)^2} - \frac{m_{b[c]}(m_d - 3m_u)}{128\pi^2(q^2 - m_{b[c]}^2)} \Big] \\
&- m_0^2\langle\bar{d}d\rangle\frac{3m_{b[c]} + 4m_d}{96\pi^2(m_{b[c]}^2 - q^2)} + m_0^2\langle\bar{u}u\rangle\frac{9m_{b[c]} + 3m_d - 7m_u}{96\pi^2(m_{b[c]}^2 - q^2)} \Big\} \Theta[L_1(s, s', q^2)] \\
&+ \int_0^1 dx \int_0^{1-x} dy \left\{ \frac{1}{8\pi^2u} \left[ \langle\bar{d}d\rangle \left( m_{b[c]} - 2m_{b[c]}x - m_uu + m_d(3x - 1)(y + u) \right) \right. \right. \\
&+ \langle\bar{u}u\rangle \left( m_{b[c]} - 2m_{b[c]}x - 4m_du - 2m_u(y - 3xy - 3xu) \right) \Big] + \langle\alpha_s\frac{G^2}{\pi}\rangle \frac{1}{96\pi^2u^3} \\
&\times \left[ 3u^2(3x - 1)(y + u) + xy(1 - y + x(3x + 6y - 4)) \right] \Big\} \Theta[L_2(s, s', q^2)], \tag{17}
\end{aligned}$$

where

$$\begin{aligned}
L_1(s, s', q^2) &= s', \\
L_2(s, s', q^2) &= -m_{b[c]}^2x + sx - sx^2 + s'y + q^2xy - sxy - s'xy - s'y^2, \\
u &= x + y - 1, \tag{18}
\end{aligned}$$

with  $\Theta[\dots]$  being the unit-step function.

As we previously mentioned, the QCD sum rules for the strong form factors are obtained by matching the hadronic and OPE sides of the correlation function. As a result, for  $\gamma_5$  structure, we get

$$\begin{aligned}
g_{\Lambda_b NB[\Lambda_c ND]}(q^2) &= -e^{\frac{m_{\Lambda_b[\Lambda_c]}^2}{M^2}} e^{\frac{m_N^2}{M'^2}} \frac{(m_{b[c]} + m_u)(q^2 - m_{B[D]}^2)}{m_{B[D]}^2 f_{B[D]} \lambda_{\Lambda_b[\Lambda_c]}^\dagger \lambda_N (m_N m_{\Lambda_b[\Lambda_c]} - m_{\Lambda_b[\Lambda_c]}^2)} \\
&\times \left\{ \int_{(m_{b[c]} + m_u + m_d)^2}^{s_0} ds \int_{(2m_u + m_d)^2}^{s'_0} ds' e^{-\frac{s}{M^2}} e^{-\frac{s'}{M'^2}} \left[ \rho_1^{pert}(s, s', q^2) + \rho_1^{non-pert}(s, s', q^2) \right] \right\}, \tag{19}
\end{aligned}$$

where  $s_0$  and  $s'_0$  are continuum thresholds in  $\Lambda_b[\Lambda_c]$  and  $N$  channels, respectively.

### 3 Numerical results

This section contains the numerical analysis of the obtained sum rules for the strong coupling form factors including their behavior in terms of  $Q^2 = -q^2$ . For the analysis, we use the input parameters given in table 1.

Parameters	Values
$m_b$	$(4.18 \pm 0.03) \text{ GeV}$ [37]
$m_c$	$(1.275 \pm 0.025) \text{ GeV}$ [37]
$m_d$	$4.8_{-0.3}^{+0.5} \text{ MeV}$ [37]
$m_u$	$2.3_{-0.5}^{+0.7} \text{ MeV}$ [37]
$m_B$	$(5279.26 \pm 0.17) \text{ MeV}$ [37]
$m_D$	$(1864.84 \pm 0.07) \text{ MeV}$ [37]
$m_N$	$(938.272046 \pm 0.000021) \text{ MeV}$ [37]
$m_{\Lambda_b}$	$(5619.5 \pm 0.4) \text{ MeV}$ [37]
$m_{\Lambda_c}$	$(2286.46 \pm 0.14) \text{ MeV}$ [37]
$f_B$	$(248 \pm 23_{exp} \pm 25_{Vub}) \text{ MeV}$ [38]
$f_D$	$(205.8 \pm 8.5 \pm 2.5) \text{ MeV}$ [39]
$\lambda_N^2$	$0.0011 \pm 0.0005 \text{ GeV}^6$ [40]
$\lambda_{\Lambda_b}$	$(3.85 \pm 0.56)10^{-2} \text{ GeV}^3$ [22]
$\lambda_{\Lambda_c}$	$(3.34 \pm 0.47)10^{-2} \text{ GeV}^3$ [22]
$\langle \bar{u}u \rangle (1 \text{ GeV}) = \langle \bar{d}d \rangle (1 \text{ GeV})$	$-(0.24 \pm 0.01)^3 \text{ GeV}^3$ [41]
$\langle \frac{\alpha_s G^2}{\pi} \rangle$	$(0.012 \pm 0.004) \text{ GeV}^4$ [42]
$m_0^2 (1 \text{ GeV})$	$(0.8 \pm 0.2) \text{ GeV}^2$ [42]

Table 1: Input parameters used in calculations.

The analysis starts by the determination of the working regions for the auxiliary parameters  $M^2$ ,  $M'^2$ ,  $s_0$  and  $s'_0$ . These parameters, which arise due to the double Borel transformation and continuum subtraction, are not physical parameters so the strong coupling form factors should be almost independent of these parameters. Being related to the energy of the first excited states in the initial and final channels, the continuum thresholds are not completely arbitrary. The continuum thresholds  $s_0$  and  $s'_0$  are the energy squares which characterize the beginning of the continuum. If we denote the ground states masses in the initial and final channels respectively by  $m$  and  $m'$ , the quantities  $\sqrt{s_0} - m$  and  $\sqrt{s'_0} - m'$  are the energies needed to excite the particles to their first excited states with the same quantum numbers. The  $\sqrt{s_0} - m$  and  $\sqrt{s'_0} - m'$  are well known for the states under consideration [37], where they lie roughly between 0.1 GeV and 0.3 GeV. These values lead to the working intervals of the continuum thresholds as  $32.7[5.7] \text{ GeV}^2 \leq s_0 \leq 34.5[6.7] \text{ GeV}^2$  and  $1.08 \text{ GeV}^2 \leq s'_0 \leq 1.56 \text{ GeV}^2$  for the strong vertex  $\Lambda_b NB[\Lambda_c ND]$ .

In the determination of the working regions of Borel parameters  $M^2$  and  $M'^2$ , one considers the pole dominance as well as the convergence of the OPE. In technique language, the upper bounds on these parameters are obtained by requiring that the pole contribution

exceeds the contributions of the higher states and continuum, i.e. the condition

$$\frac{\int_{s_0}^{\infty} ds \int_{s'_0}^{\infty} ds' e^{-\frac{s}{M^2}} e^{-\frac{s'}{M'^2}} \rho_i(s, s', Q^2)}{\int_{s_{min}}^{\infty} ds \int_{s'_{min}}^{\infty} ds' e^{-\frac{s}{M^2}} e^{-\frac{s'}{M'^2}} \rho_i(s, s', Q^2)} < 1/3, \quad (20)$$

should be satisfied, where for each structure  $\rho_i(s, s', Q^2) = \rho_i^{pert}(s, s', Q^2) + \rho_i^{non-pert}(s, s', Q^2)$ ,  $s_{min} = (m_{b[c]} + m_u + m_d)^2$  and  $s'_{min} = (2m_u + m_d)^2$ . The lower bounds on  $M^2$  and  $M'^2$  are obtained by demanding that the contribution of the perturbative part exceeds the non-perturbative contributions. These considerations lead to the windows  $10[2] \text{ GeV}^2 \leq M^2 \leq 20[6] \text{ GeV}^2$  and  $1 \text{ GeV}^2 \leq M'^2 \leq 3 \text{ GeV}^2$  for the Borel mass parameters corresponding to the strong vertex  $\Lambda_b NB[\Lambda_c ND]$  in which our results have weak dependencies on the Borel mass parameters (see figures 1-2).

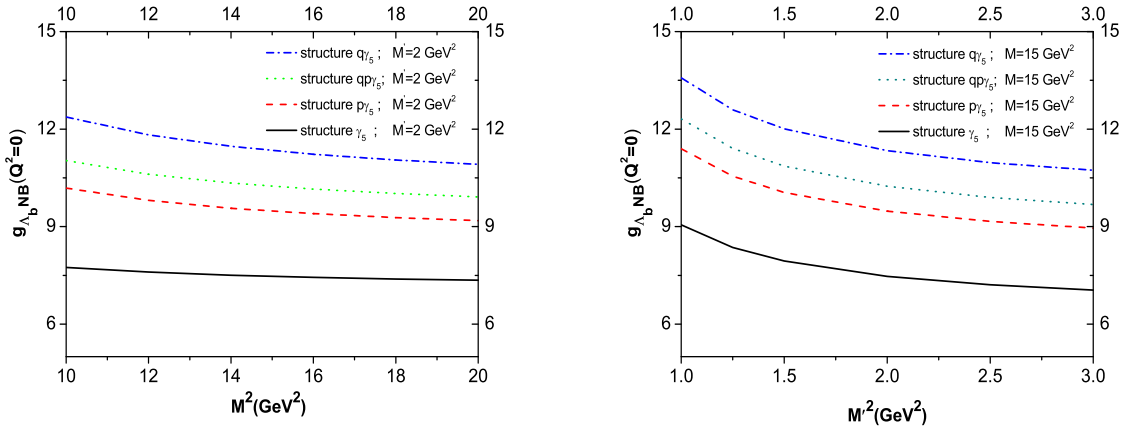


Figure 1: **Left:**  $g_{\Lambda_b NB}(Q^2 = 0)$  as a function of the Borel mass  $M^2$  at average values of continuum thresholds. **Right:**  $g_{\Lambda_b NB}(Q^2 = 0)$  as a function of the Borel mass  $M'^2$  at average values of continuum thresholds.

Now, we use the working regions of auxiliary parameters as well as values of other input parameters to find out the dependency of the strong coupling form factors on  $Q^2$ . Our numerical calculations reveal that the following fit function well describes the strong coupling form factors in terms of  $Q^2$ :

$$g_{\Lambda_b NB[\Lambda_c ND]}(Q^2) = c_1 \exp \left[ -\frac{Q^2}{c_2} \right] + c_3, \quad (21)$$

where the values of the parameters  $c_1$ ,  $c_2$  and  $c_3$  for different structures are presented in tables 2 and 3 for  $\Lambda_b NB$  and  $\Lambda_c ND$ , respectively. In figure 3, we depict the dependence of the strong coupling form factors on  $Q^2$  at average values of the continuum thresholds and Borel mass parameters for both the QCD sum rules and fitting results. From this figure, we see that the QCD sum rules are truncated at some points at negative values of  $Q^2$  and the fitting results coincide well with the sum rules predictions up to these points.



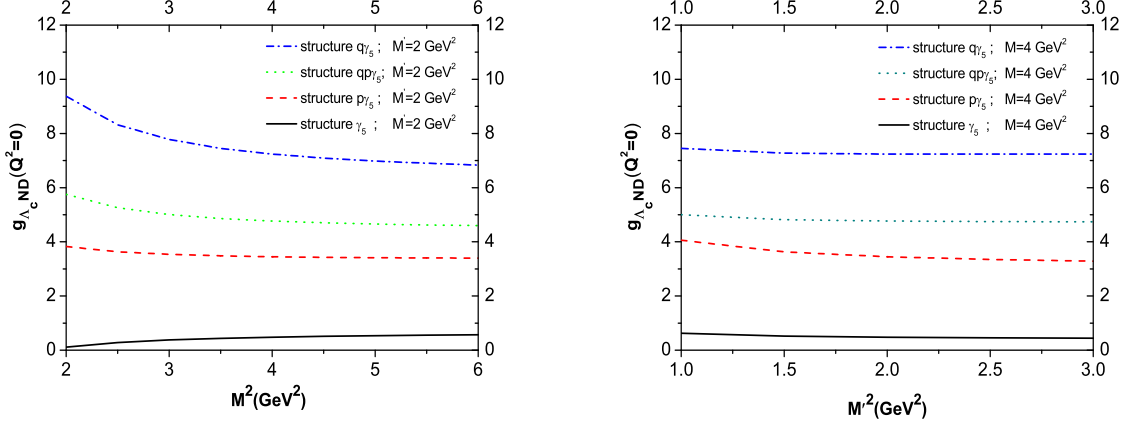


Figure 2: The same as figure 1 but for  $g_{\Lambda_c ND}(Q^2 = 0)$ .

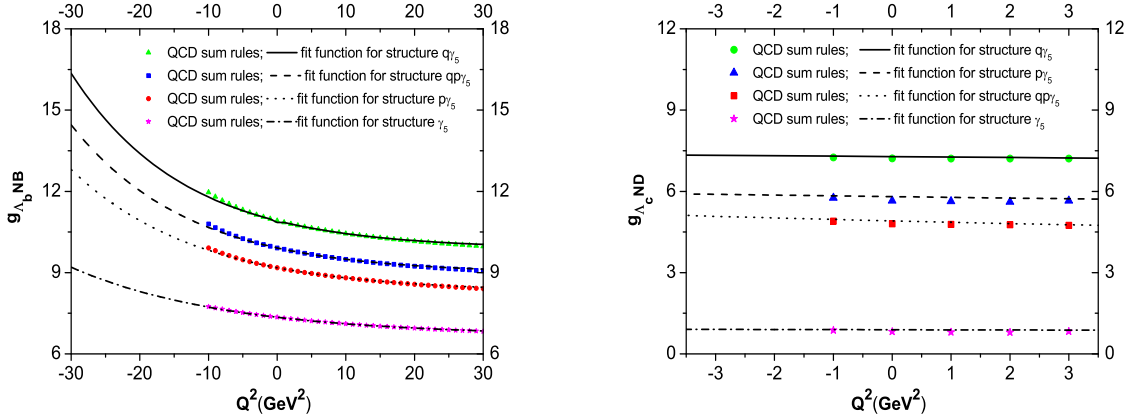


Figure 3: **Left:**  $g_{\Lambda_b NB}(Q^2)$  as a function of  $Q^2$  at average values of the continuum thresholds and Borel mass parameters. **Right:**  $g_{\Lambda_c ND}(Q^2)$  as a function of  $Q^2$  at average values of the continuum thresholds and Borel mass parameters.

The values of the strong coupling constants obtained from the fit function at  $Q^2 = -m_{B[D]}^2$  for all structures are given in table 4. The errors appearing in the results are due to the uncertainties of the input parameters and those coming from the calculations of the working regions for the auxiliary parameters. From table 4, we see that all structures except that  $\gamma_5$  lead to very close results. We also depict the average of the coupling constants under consideration, obtained from all the structures used, in table 4.

At this stage, we compare our result of the coupling constant  $g_{\Lambda_c ND}$  obtained at  $Q^2 = 0$  with that of Ref. [19] for the Dirac structure  $\not{q}\gamma_5$ . At  $Q^2 = 0$ , we get the result  $g_{\Lambda_c ND} = 7.28 \pm 2.18$  for this structure, which is consistent with the prediction of [19], i.e.,  $g_{\Lambda_c ND} = \sqrt{4\pi}(1.9 \pm 0.6) = 6.74 \pm 2.12$  within the errors.

To summarize, we have calculated the strong coupling constants  $g_{\Lambda_b NB}$  and  $g_{\Lambda_c ND}$  in the framework of the three-point QCD sum rules. Our results can be used in the bottom and charmed mesons clouds description of the nucleon which may be used to explain exotic

structure	$c_1$	$c_2(\text{GeV}^2)$	$c_3$
$\gamma_5$	$0.69 \pm 0.21$	$22.96 \pm 6.66$	$6.67 \pm 2.00$
$\not{p}\gamma_5$	$0.90 \pm 0.27$	$18.60 \pm 5.58$	$8.28 \pm 2.32$
$\not{q}\gamma_5$	$1.04 \pm 0.31$	$16.40 \pm 4.92$	$9.87 \pm 2.67$
$\not{q}\not{p}\gamma_5$	$0.95 \pm 0.28$	$17.10 \pm 4.79$	$8.96 \pm 2.69$

Table 2: Parameters appearing in the fit function of the coupling form factor for  $\Lambda_b NB$  vertex.

structure	$c_1$	$c_2(\text{GeV}^2)$	$c_3$
$\gamma_5$	$-0.08 \pm 0.02$	$-17.74 \pm 4.79$	$0.97 \pm 0.29$
$\not{p}\gamma_5$	$-9.01 \pm 2.70$	$-328.82 \pm 98.65$	$14.81 \pm 4.00$
$\not{q}\gamma_5$	$-20.04 \pm 5.81$	$-1221.76 \pm 366.53$	$27.32 \pm 8.20$
$\not{q}\not{p}\gamma_5$	$0.86 \pm 0.26$	$16.63 \pm 4.82$	$4.05 \pm 1.22$

Table 3: Parameters appearing in the fit function of the coupling form factor for  $\Lambda_c ND$  vertex.

events observed by different experiments. The obtained results can also be used in analysis of the results of heavy ion collision experiments like  $\overline{P}ANDA$  at FAIR. These results may also be used in exact determinations of the modifications in the masses, decay constants and other parameters of the  $B$  and  $D$  mesons in nuclear medium.

## 4 Acknowledgment

This work has been supported in part by the Scientific and Technological Research Council of Turkey (TUBITAK) under the research project 114F018.

## References

- [1] D. W. Wang, M. Q. Huang, Phys. Rev. D 68, 034019 (2003).
- [2] Z. G. Wang, Eur. Phys. J. C 54, 231 (2008).
- [3] F. O. Duraes, M. Nielsen, Phys. Lett. B 658, 40 (2007).
- [4] X. Liu, H. X. Chen, Y. R. Liu, A. Hosaka, S. L. Zhu, Phys. Rev. D 77, 014031 (2008).
- [5] D. W. Wang, M. Q. Huang, C. Z. Li, Phys. Rev. D 65, 094036 (2002).

structure	$g_{\Lambda_b NB}(Q^2 = -m_B^2)$	$g_{\Lambda_c ND}(Q^2 = -m_D^2)$
$\gamma_5$	$8.97 \pm 2.69$	$0.91 \pm 0.27$
$\not{p}\gamma_5$	$12.31 \pm 3.57$	$5.90 \pm 1.77$
$\not{q}\gamma_5$	$15.57 \pm 4.67$	$7.34 \pm 2.20$
$\not{q}\not{p}\gamma_5$	$13.81 \pm 4.14$	$5.11 \pm 1.53$
average	$12.67 \pm 3.76$	$4.82 \pm 1.44$

Table 4: Values of the  $g_{\Lambda_b NB}$  and  $g_{\Lambda_c ND}$  coupling constants for different structures.

- [6] N. Mathur, R. Lewis, R. M. Woloshyn, Phys. Rev. D 66, 014502 (2002).
- [7] D. Ebert, R. N. Faustov, V. O. Galkin, Phys. Rev. D 72, 034026 (2005).
- [8] M. Karliner, H. J. Lipkin, Phys. Lett. B 660, 539 (2008).
- [9] M. Karliner, B. Keren-Zur, H. J. Lipkin, J. L. Rosner, arXiv:0706.2163 (2007).
- [10] J. L. Rosner, Phys. Rev. D 75, 013009 (2007).
- [11] T. M. Aliev, K. Azizi, A. Ozpineci, Nucl. Phys. B 808, 137 (2009).
- [12] B. Julia-Diaz, D. O. Riska, Nucl. Phys. A 739, 69 (2004).
- [13] S. Scholl, H. Weigel, Nucl. Phys. A 735, 163 (2004).
- [14] A. Faessler et. al, Phys. Rev. D 73, 094013 (2006).
- [15] B. Patel, A. K. Rai, P. C. Vinodkumar, Frascati Physics Series Vol. XLVI (2007), arXiv: 0803.0221.
- [16] C. S. An, Nucl. Phys. A 797, 131 (2007), Erratum-ibid; A 801, 82 (2008).
- [17] T. M. Aliev, A. Ozpineci, M. Savci, Phys. Rev. D 65, 096004 (2002).
- [18] T. M. Aliev, K. Azizi, A. Ozpineci, Phys. Rev. D 79, 056005 (2009).
- [19] F. S. Navarra, M. Nielsen, Phys. Lett. B 443, 285 (1998).
- [20] P.-Z. Huang, H.-X. Chen, S.-L. Zhu, Phys. Rev. D 80, 094007 (2009).
- [21] Z.-G. Wang, Eur. Phys. J. A 44, 105 (2010); Phys. Rev. D 81, 036002 (2010).
- [22] K. Azizi, M. Bayar, A. Ozpineci, Phys. Rev. D 79, 056002 (2009).
- [23] T. M. Aliev, K. Azizi, M. Savci, Phys. Lett. B 696, 220 (2011).
- [24] H.-Y. Cheng, C.-K. Chua, Phys. Rev. D 75, 014006 (2007).

- [25] A. Khodjamirian, Ch. Klein, Th. Mannel, Y.-M. Wang, JHEP 1109, 106 (2011).
- [26] E. Hernandez, J. Nieves, Phys. Rev. D 84, 057902 (2011).
- [27] K. Azizi, M. Bayar, Y. Sarac and H. Sundu, Phys. Rev. D 80, 096007 (2009).
- [28] T. Gutsche, M. A. Ivanov, J. G. Korner, V. E. Lyubovitskij, P. Santorelli, arXiv:1410.6043 (2014).
- [29] M. A. Shifman, A. I. Vainshtein, V. I. Zakharov, Nucl. Phys. B147, 385 (1979); Nucl. Phys. B 147, 448 (1979).
- [30] K. Azizi, N. Er, H. Sundu, Eur. Phys. J. C 74, 3021 (2014).
- [31] A. Kumar, Advances in High Energy Physics 2014, 549726 (2014).
- [32] Z.-G. Wang, T. Huang, Phys. Rev. C 84, 048201 (2011).
- [33] Z.-G. Wang, Int. J. Mod. Phys. A 28, 1350049 (2013).
- [34] A. Hayashigaki, Phys. Lett. B 487, 96 (2000).
- [35] S. Choe, M. K. Cheoun, S. H. Lee, Phys. Rev. C 53, 1363 (1996).
- [36] L. J. Reinders, H. Rubinstein and S. Yazaki, Phys. Rept. 127, 1 (1985).
- [37] K. A. Olive et al. (Particle Data Group), Chin. Phys. C, 38, 090001 (2014).
- [38] A. Khodjamirian, “B and D Meson Decay Constant in QCD”, Lecture 1 at “3rd Belle Analysis School”, Sept. 22, 2010, KEK.
- [39] B. I. Eisenstein et al. (CLEO Collab.), Phys. Rev. D78, 052003 (2008).
- [40] K. Azizi, N. Er, Eur. Phys. J. C74, 2904 (2014).
- [41] B. L. Ioffe, Prog. Part. Nucl. Phys. 56, 232 (2006).
- [42] V. M. Belyaev, B. L. Ioffe, Sov. Phys. JETP 57, 716 (1982); Phys. Lett. B 287, 176 (1992).